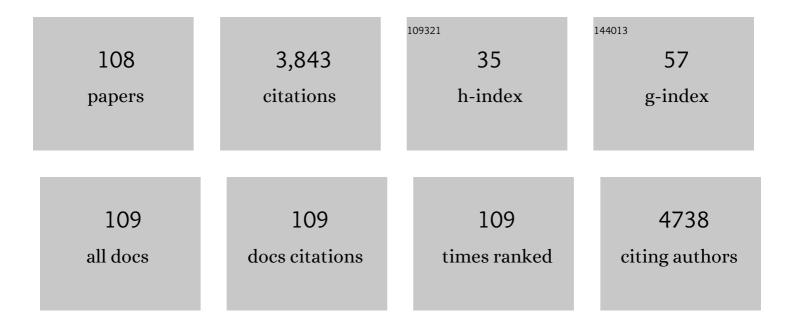
Pingchuan Sun

List of Publications by Year in descending order

Source: https://exaly.com/author-pdf/5078380/publications.pdf Version: 2024-02-01



Ρινορημαν διιν

#	Article	IF	CITATIONS
1	Hierarchically porous Fe/N/S/C nanospheres with high-content of Fe-Nx for enhanced ORR and Zn-air battery performance. Green Energy and Environment, 2023, 8, 1693-1702.	8.7	15
2	In-situ growth of cobalt manganate spinel nanodots on carbon black toward high-performance zinc-air battery: Dual functions of 3-aminopropyltriethoxysilane. Journal of Colloid and Interface Science, 2022, 608, 386-395.	9.4	6
3	Room temperature tunable multicolor phosphorescent polymers for humidity detection and information encryption. RSC Advances, 2022, 12, 8145-8153.	3.6	5
4	Achieving long lifetime of room-temperature phosphorescence <i>via</i> constructing vitrimer networks. Materials Chemistry Frontiers, 2022, 6, 1068-1078.	5.9	8
5	Probing the Dynamic Structural Evolution of End-Functionalized Polybutadiene/Organo-Clay Nanocomposite Gels before and after Yielding by Nonlinear Rheology and 1H Double-Quantum NMR. Polymers, 2022, 14, 1518.	4.5	2
6	Efficient oxidative-adsorptive desulfurization over highly dispersed molybdenum oxide supported on hierarchically mesoporous silica. Colloids and Surfaces A: Physicochemical and Engineering Aspects, 2022, 645, 128922.	4.7	1
7	Steam-assisted strategy to fabricate Anatase-free hierarchical titanium Silicalite-1 Single-Crystal for oxidative desulfurization. Journal of Colloid and Interface Science, 2022, 617, 32-43.	9.4	14
8	Hierarchically Porous Mesostructured Polydopamine Nanospheres and Derived Carbon for Supercapacitors. Langmuir, 2022, 38, 8964-8974.	3.5	4
9	High-performance ionic conductive poly(vinyl alcohol) hydrogels for flexible strain sensors based on a universal soaking strategy. Materials Chemistry Frontiers, 2021, 5, 315-323.	5.9	51
10	Antifogging and antibacterial properties of amphiphilic coatings based on zwitterionic copolymers. Science China Technological Sciences, 2021, 64, 817-826.	4.0	11
11	Bioinspired, nucleobase-driven, highly resilient, and fast-responsive antifreeze ionic conductive hydrogels for durable pressure and strain sensors. Journal of Materials Chemistry A, 2021, 9, 20703-20713.	10.3	55
12	Fluorescent, electrically responsive and ultratough self-healing hydrogels <i>via</i> bioinspired all-in-one hierarchical micelles. Materials Horizons, 2021, 8, 3096-3104.	12.2	21
13	Bioinspired Polyurethane Using Multifunctional Block Modules with Synergistic Dynamic Bonds. ACS Macro Letters, 2021, 10, 510-517.	4.8	36
14	Heterogeneous Dynamics and Microdomain Structure of High-Performance Chitosan Film as Revealed by Solid-State NMR. Journal of Physical Chemistry C, 2021, 125, 13572-13580.	3.1	8
15	Supramolecular Polydimethylsiloxane Elastomer with Enhanced Mechanical Properties and Self-Healing Ability Engineered by Synergetic Dynamic Bonds. ACS Applied Polymer Materials, 2021, 3, 3373-3382.	4.4	31
16	Hierarchically porous silica supported ceria and platinum nanoparticles for catalytic combustion of toluene. Journal of Alloys and Compounds, 2021, 867, 159030.	5.5	10
17	Effects of rare earth metal doping on Au/ReZrO ₂ catalysts for efficient hydrogen generation from formic acid. New Journal of Chemistry, 2021, 45, 5704-5711.	2.8	5
18	Encapsulated FeP nanoparticles with in-situ formed P-doped graphene layers: Boosting activity in oxygen reduction reaction. Science China Materials, 2021, 64, 1159-1172.	6.3	19

#	Article	IF	CITATIONS
19	Bioinspired tough, conductive hydrogels with thermally reversible adhesiveness based on nanoclay confined NIPAM polymerization and a dopamine modified polypeptide. Materials Chemistry Frontiers, 2020, 4, 189-196.	5.9	33
20	Highly Bidirectional Bendable Actuator Engineered by LCST–UCST Bilayer Hydrogel with Enhanced Interface. ACS Applied Materials & Interfaces, 2020, 12, 55290-55298.	8.0	89
21	Platinum Nanoparticles Supported on Hierarchically Porous Aluminosilicate Nanospheres for Low-Temperature Catalytic Combustion of Volatile Organic Compounds. ACS Applied Nano Materials, 2020, 3, 8472-8482.	5.0	12
22	A general approach for hierarchically porous metal/N/C nanosphere electrocatalysts: nano-confined pyrolysis of <i>in situ</i> -formed amorphous metal–ligand complexes. Journal of Materials Chemistry A, 2020, 8, 21026-21035.	10.3	20
23	Hierarchical Dynamics in a Transient Polymer Network Cross-Linked by Orthogonal Dynamic Bonds. Macromolecules, 2020, 53, 5937-5949.	4.8	29
24	Polyelectrolyte–Surfactant Mesomorphous Complex Templating: A Versatile Approach for Hierarchically Porous Materials. Langmuir, 2020, 36, 1851-1863.	3.5	26
25	Mechanically strong and tough hydrogels with pH-triggered self-healing and shape memory properties based on a dual physically crosslinked network. Polymer Chemistry, 2020, 11, 1906-1918.	3.9	30
26	Optimized Enhancement Effect of Sulfur in Fe–N–S Codoped Carbon Nanosheets for Efficient Oxygen Reduction Reaction. ACS Applied Materials & Interfaces, 2020, 12, 23995-24006.	8.0	48
27	Dual Crossâ€linked Vinyl Vitrimer with Efficient Selfâ€Catalysis Achieving Tripleâ€Shapeâ€Memory Properties. Macromolecular Rapid Communications, 2019, 40, e1900313.	3.9	38
28	Cation-induced chirality in a bifunctional metal-organic framework for quantitative enantioselective recognition. Nature Communications, 2019, 10, 5117.	12.8	150
29	Customizable Multidimensional Self-Wrinkling Structure Constructed via Modulus Gradient in Chitosan Hydrogels. Chemistry of Materials, 2019, 31, 10032-10039.	6.7	55
30	Hierarchically Mesoporous Titanosilicate Single-Crystalline Nanospheres for Room Temperature Oxidative–Adsorptive Desulfurization. ACS Applied Nano Materials, 2019, 2, 6602-6610.	5.0	25
31	Hierarchically Porous Silica Prepared with Anionic Polyelectrolyte–Nonionic Surfactant Mesomorphous Complex as Dynamic Template. ACS Omega, 2019, 4, 1443-1448.	3.5	3
32	Poly(N-isopropylacrylamide)/polydopamine/clay nanocomposite hydrogels with stretchability, conductivity, and dual light- and thermo- responsive bending and adhesive properties. Colloids and Surfaces B: Biointerfaces, 2019, 177, 149-159.	5.0	45
33	Using Dynamic Bonds to Enhance the Mechanical Performance: From Microscopic Molecular Interactions to Macroscopic Properties. Macromolecules, 2019, 52, 5014-5025.	4.8	64
34	High-performance polyurethane nanocomposites based on UPy-modified cellulose nanocrystals. Carbohydrate Polymers, 2019, 219, 191-200.	10.2	37
35	Bio-inspired self-healing polyurethanes with multiple stimulus responsiveness. Polymer Chemistry, 2019, 10, 3362-3370.	3.9	29
36	Using Zn ²⁺ lonomer To Catalyze Transesterification Reaction in Epoxy Vitrimer. Industrial & Engineering Chemistry Research, 2019, 58, 5698-5706.	3.7	67

#	Article	IF	CITATIONS
37	Highly efficient photothermal nanoagent achieved by harvesting energy via excited-state intramolecular motion within nanoparticles. Nature Communications, 2019, 10, 768.	12.8	296
38	Artificial spider silk from ion-doped and twisted core-sheath hydrogel fibres. Nature Communications, 2019, 10, 5293.	12.8	123
39	Ultrafine PdAu nanoparticles immobilized on amine functionalized carbon black toward fast dehydrogenation of formic acid at room temperature. Nanoscale Advances, 2019, 1, 4415-4421.	4.6	24
40	Strain-induced structural and dynamic changes in segmented polyurethane elastomers. Polymer, 2019, 163, 154-161.	3.8	31
41	Multiple-responsive shape memory polyacrylonitrile/graphene nanocomposites with rapid self-healing and recycling properties. RSC Advances, 2018, 8, 1225-1231.	3.6	25
42	Robust Anisotropic Cellulose Hydrogels Fabricated via Strong Self-aggregation Forces for Cardiomyocytes Unidirectional Growth. Chemistry of Materials, 2018, 30, 5175-5183.	6.7	137
43	High-performance recyclable cross-linked polyurethane with orthogonal dynamic bonds: The molecular design, microstructures, and macroscopic properties. Polymer, 2018, 148, 127-137.	3.8	48
44	Conformations and Intermolecular Interactions in Cellulose/Silk Fibroin Blend Films: A Solid-State NMR Perspective. Journal of Physical Chemistry B, 2017, 121, 6108-6116.	2.6	47
45	Rapid self-healing and recycling of multiple-responsive mechanically enhanced epoxy resin/graphene nanocomposites. RSC Advances, 2017, 7, 46336-46343.	3.6	23
46	Versatile multicompartment nanoparticles constructed with two thermo-responsive, pH-responsive and hydrolytic diblock copolymers. Polymer Chemistry, 2017, 8, 5593-5602.	3.9	10
47	Viscoelasticity and Structures in Chemically and Physically Dual-Cross-Linked Hydrogels: Insights from Rheology and Proton Multiple-Quantum NMR Spectroscopy. Macromolecules, 2017, 50, 9340-9352.	4.8	59
48	Spectroscopic Analysis of Epoxy/Block-Copolymer Blends. , 2017, , 919-953.		0
49	2H Solid-State NMR Analysis of the Dynamics and Organization of Water in Hydrated Chitosan. Polymers, 2016, 8, 149.	4.5	13
50	Entropy effect of alkyl tails on phase behaviors of side-chain-jacketed polyacetylenes: Columnar phase and isotropic phase reentry. Polymer, 2016, 87, 260-267.	3.8	7
51	Comparative analysis of the interaction of capecitabine and gefitinib with human serum albumin using 19 F nuclear magnetic resonance-based approach. Journal of Pharmaceutical and Biomedical Analysis, 2016, 129, 15-20.	2.8	14
52	Molecular origin of the shape memory properties of heat-shrink crosslinked polymers as revealed by solid-state NMR. Polymer, 2016, 107, 61-70.	3.8	19
53	Binding mechanism of the tyrosine-kinase inhibitor nilotinib to human serum albumin determined by 1 H STD NMR, 19 F NMR, and molecular modeling. Journal of Pharmaceutical and Biomedical Analysis, 2016, 124, 1-9.	2.8	15
54	Reversible Interactions of Proteins with Mixed Shell Polymeric Micelles: Tuning the Surface Hydrophobic/Hydrophilic Balance toward Efficient Artificial Chaperones. Langmuir, 2016, 32, 2737-2749.	3.5	20

#	Article	IF	CITATIONS
55	Spectroscopic Analysis of Epoxy/Block Copolymer Blends. , 2016, , 1-35.		ο
56	Effect of PEO molecular weight on the miscibility and dynamics in epoxy/PEO blends. European Physical Journal E, 2015, 38, 118.	1.6	7
57	A Single Molecular Diels–Alder Crosslinker for Achieving Recyclable Cross‣inked Polymers. Macromolecular Rapid Communications, 2015, 36, 1687-1692.	3.9	52
58	Low temperature oxidative desulfurization with hierarchically mesoporous titaniumsilicate Ti-SBA-2 single crystals. Chemical Communications, 2015, 51, 11500-11503.	4.1	58
59	Macro-RAFT agent mediated dispersion copolymerization: a small amount of solvophilic co-monomer leads to a great change. Polymer Chemistry, 2015, 6, 4911-4920.	3.9	45
60	Mg ²⁺ -assisted low temperature reduction of alloyed AuPd/C: an efficient catalyst for hydrogen generation from formic acid at room temperature. Chemical Communications, 2015, 51, 10887-10890.	4.1	34
61	Phase cycling schemes for finite-pulse-RFDR MAS solid state NMR experiments. Journal of Magnetic Resonance, 2015, 252, 55-66.	2.1	43
62	Hydrogenation induced deviation of temperature and concentration dependences of polymer-solvent interactions in poly(vinyl chloride) and a new eco-friendly plasticizer. European Physical Journal Plus, 2015, 130, 1.	2.6	2
63	Probing the Nanostructure, Interfacial Interaction, and Dynamics of Chitosan-Based Nanoparticles by Multiscale Solid-State NMR. ACS Applied Materials & Interfaces, 2014, 6, 21397-21407.	8.0	21
64	B 3Q MAS NMR Study on Glucoseâ€Responsive Micelles Selfâ€assembled from PEGâ€ <i>b</i> â€P(AAâ€ <i>co</i> â€AAPBA). Chinese Journal of Chemistry, 2014, 32, 97-102.	4.9	3
65	A New Strategy To Synthesize Temperature- and pH-Sensitive Multicompartment Block Copolymer Nanoparticles by Two Macro-RAFT Agents Comediated Dispersion Polymerization. Macromolecules, 2014, 47, 7442-7452.	4.8	47
66	Au–Pd alloy catalyst with high performance for hydrogen generation from formic acid-formate solution at nearly 0 °C. RSC Advances, 2014, 4, 44500-44503.	3.6	20
67	Synergy between Polyamine and Anionic Surfactant: A Bioinspired Approach for Ordered Mesoporous Silica. Langmuir, 2014, 30, 2329-2334.	3.5	4
68	Reversible Cross-Linking, Microdomain Structure, and Heterogeneous Dynamics in Thermally Reversible Cross-Linked Polyurethane as Revealed by Solid-State NMR. Journal of Physical Chemistry B, 2014, 118, 1126-1137.	2.6	58
69	Unique Interphase and Cross-Linked Network Controlled by Different Miscible Blocks in Nanostructured Epoxy/Block Copolymer Blends Characterized by Solid-State NMR. Journal of Physical Chemistry C, 2014, 118, 13285-13299.	3.1	34
70	Facile one-step room-temperature synthesis of Mn-based spinel nanoparticles for electro-catalytic oxygen reduction. RSC Advances, 2014, 4, 4727-4731.	3.6	27
71	The strong interaction between poly(vinyl chloride) and a new eco-friendly plasticizer: A combined experiment and calculation study. Polymer, 2014, 55, 2831-2840.	3.8	13
72	Critical Effect of Segmental Dynamics in Polybutadiene/Clay Nanocomposites Characterized by Solid State ¹ H NMR Spectroscopy. Journal of Physical Chemistry C, 2014, 118, 5606-5614.	3.1	34

#	Article	IF	CITATIONS
73	Dynamic polymer brushes on the surface of silica particles. RSC Advances, 2013, 3, 7023.	3.6	15
74	Bioâ€Inspired Highâ€Performance and Recyclable Crossâ€Linked Polymers. Advanced Materials, 2013, 25, 4912-4917.	21.0	224
75	Hydrophilic interface-crosslinked polymer micelles: a platform for nanoreactors and nanocarriers. Polymer Chemistry, 2013, 4, 4499.	3.9	6
76	Hierarchically mesoporous silica single-crystalline nanorods with three dimensional cubic Fm-3m mesostructure. Journal of Materials Chemistry A, 2013, 1, 14555.	10.3	24
77	RAFTâ€mediated emulsion polymerization of styrene using brush copolymer as surfactant macroâ€RAFT agent: Effect of the brush copolymer sequence and chemical composition. Journal of Polymer Science Part A, 2013, 51, 1147-1161.	2.3	30
78	Heterogeneity, Segmental and Hydrogen Bond Dynamics, and Aging of Supramolecular Self-Healing Rubber. Macromolecules, 2013, 46, 1841-1850.	4.8	89
79	Confinement-Induced Deviation of Chain Mobility and Glass Transition Temperature for Polystyrene/Au Nanoparticles. Macromolecules, 2013, 46, 2292-2297.	4.8	50
80	Efficient Synthesis of Molecularly Imprinted Polymers with Enzyme Inhibition Potency by the Controlled Surface Imprinting Approach. ACS Macro Letters, 2013, 2, 566-570.	4.8	69
81	Interface cross-linked polymeric micelles with mixed coronal chains prepared by RAFT polymerization at the interface. Soft Matter, 2012, 8, 11809.	2.7	14
82	Accessing Structure and Dynamics of Mobile Phase in Organic Solids by Real-Time T _{1C} Filter PISEMA NMR Spectroscopy. Journal of Physical Chemistry A, 2012, 116, 979-984.	2.5	9
83	Investigation on the artificial exchange signals induced by the RIDER effect in CODEX experiments. Solid State Nuclear Magnetic Resonance, 2012, 47-48, 28-34.	2.3	1
84	RAFTâ€mediated batch emulsion polymerization of styrene using poly[<i>N</i> â€(4â€vinylbenzyl)â€ <i>N</i> , <i>N</i> â€dibutylamine hydrochloride] trithiocarbonate as both surfactant and macroâ€RAFT agent. Journal of Polymer Science Part A, 2012, 50, 2484-2498.	2.3	22
85	Tracking the interdiffusion of polymers at a molecular level by ¹ H dipolar filter solid-state NMR under fast magic angle spinning. Soft Matter, 2011, 7, 691-697.	2.7	13
86	Efficient Identification of Different Types of Carbons in Organic Solids by 2D Solid-State NMR Spectroscopy. Journal of Physical Chemistry A, 2011, 115, 11665-11670.	2.5	6
87	Amphiphilic Triblock Copolymer Bioconjugates with Biotin Groups at the Junction Points: Synthesis, Self-Assembly, and Bioactivity. Macromolecules, 2011, 44, 2016-2024.	4.8	34
88	Reactive triblock copolymer micelles induced by click reaction: A platform for RAFT polymerization. Soft Matter, 2011, 7, 11194.	2.7	9
89	Solid state NMR study of hydrogen bonding, miscibility, and dynamics in multiphase polymer systems. Frontiers of Chemistry in China: Selected Publications From Chinese Universities, 2011, 6, 173-189.	0.4	5
90	Evolution of interphase in styrene-butadiene block copolymers as revealed by 1H solid-state NMR: Effect of temperature and molecular architecture. Polymer, 2010, 51, 2069-2076.	3.8	10

#	Article	IF	CITATIONS
91	Silk Fibroin/Montmorillonite Nanocomposites: Effect of pH on the Conformational Transition and Clay Dispersion. Biomacromolecules, 2010, 11, 1796-1801.	5.4	62
92	Enhanced Exfoliation of Organoclay in Partially Endâ€Functionalized Nonâ€Polar Polymer. Macromolecular Materials and Engineering, 2009, 294, 190-195.	3.6	15
93	Solid-state NMR characterization of unsaturated polyester thermoset blends containing PEO–PPO–PEO block copolymers. Polymer, 2008, 49, 2886-2897.	3.8	41
94	Probing Chain Interpenetration in Polymer Glasses by1H Dipolar Filter Solid-State NMR under Fast Magic Angle Spinning. Macromolecules, 2007, 40, 4736-4739.	4.8	28
95	Radiolaria-like Silica with Radial Spines Fabricated by a Dynamic Self-Organization. Journal of Physical Chemistry C, 2007, 111, 16544-16548.	3.1	21
96	Various Types of Hydrogen Bonds, Their Temperature Dependence and Waterâ^'Polymer Interaction in Hydrated Poly(Acrylic Acid) as Revealed by ¹ H Solid-State NMR Spectroscopy. Macromolecules, 2007, 40, 5776-5786.	4.8	66
97	Unusual Rheological Behavior of Liquid Polybutadiene Rubber/Clay Nanocomposite Gels:Â The Role of Polymerâ^'Clay Interaction, Clay Exfoliation, and Clay Orientation and Disorientation. Macromolecules, 2006, 39, 6653-6660.	4.8	64
98	Synthesis and Characterization of Mesoporous Ceria with Hierarchical Nanoarchitecture Controlled by Amino Acids. Journal of Physical Chemistry B, 2006, 110, 25782-25790.	2.6	133
99	Hierarchically helical mesostructured silica nanofibers templated by achiral cationic surfactant. Journal of Materials Chemistry, 2006, 16, 4117.	6.7	57
100	Synthesis of nanoporous silica with interior composite cells with synthetic block copolypeptide as template. Science Bulletin, 2006, 51, 493-497.	1.7	5
101	Simulated annealing study of morphological transitions of diblock copolymers in solution. Journal of Chemical Physics, 2005, 122, 204905.	3.0	47
102	Simulated annealing study of gyroid formation in diblock copolymer solutions. Physical Review E, 2005, 72, 061408.	2.1	7
103	Exfoliation of Organo-Clay in Telechelic Liquid Polybutadiene Rubber. Macromolecules, 2005, 38, 4030-4033.	4.8	49
104	Mobility, Miscibility, and Microdomain Structure in Nanostructured Thermoset Blends of Epoxy Resin and Amphiphilic Poly(ethylene oxide)-block-poly(propylene oxide)-block-poly(ethylene oxide) Triblock Copolymers Characterized by Solid-State NMR. Macromolecules, 2005, 38, 5654-5667.	4.8	77
105	Rubber/exfoliated-clay nanocomposite gel: Direct exfoliation of montmorillonite by telechelic liquid rubber. Science Bulletin, 2004, 49, 1664-1666.	1.7	5
106	Title is missing!. Journal of Porous Materials, 2003, 10, 145-150.	2.6	7
107	PGSE NMR studies of water states of hydrogel P(Am-NaA). Journal of Applied Polymer Science, 2000, 77, 424-427.	2.6	5
108	NMR characterization of absorbed water in equilibrium swollen hydrogel P(AM-NaA). Journal of Applied Polymer Science, 1999, 72, 1203-1207.	2.6	9